°C); ^{1}H NMR ($CDCl_3$) δ 2.01 (s, 3 H, CH_3), 2.41 (s, 3 H, $COCH_3$), 7.03–7.46 (m, 4 H, C_6H_4); IR (Nujol) 1750 (C=O), 1700 (C=O), 1640 (C=C), 1600 (C=C) cm^{-1}; mass spectrum, m/z 218.058 20 (calcd for $C_{12}H_{10}O_4$, 218.057 91).

(47) Mentzer, C.; Vercier, P. *Monatsh. Chem.* **1957**, *88*, 264.

Acknowledgment. We gratefully acknowledge support of this work by the National Institutes of Health (GM24254) and the donors of the Petroleum Research Fund, administered by the American Chemical Society. We also wish to thank Johnson Matthey, Inc., and Engelhard Industries for generous loans of palladium chloride.

A Model for the Cyanide Form of Oxidized Cytochrome Oxidase: An Iron(III)/Copper(II) Porphyrin Complex Displaying Ferromagnetic Coupling

Maxwell J. Gunter,*[1a] Kevin J. Berry,[1b] and Keith S. Murray*[1b]

Contribution from the Research School of Chemistry, Australian National University, Canberra 2601, Australia, and the Department of Chemistry, Monash University, Clayton, Victoria 3168, Australia. *Received June 10, 1983*

Abstract: The preparation and properties of the cyanide bridged Fe^{III}–Cu^{II} heterobinuclear complex of the ligand $\alpha,\alpha,\alpha,\alpha$-tetrakis(*o*-nicotinamidophenyl)porphyrin $[Fe(P)CNCu(N_4)](ClO_4)_2 \cdot 3H_2O$ are described. Bulk magnetic susceptibility, ESR, and Mössbauer data are interpreted in terms of weak ferromagnetic coupling between low-spin Fe(III) and Cu(II) ions, leading to an $S' = 1$ ground state with the $S' = 0$ level close in energy. A good description of the susceptibility and ESR line positions has been obtained by using the Hamiltonian $\mathcal{H} = -JS_1S_2 + J_D^{\alpha\beta}/[2\{S_1^{\alpha}S_2^{\beta} + S_1^{\beta}S_2^{\alpha}\}] + d(S_1xS_2) + [\mu_1\mu_2/r^3] - [3(\mu_1 r)(\mu_2 r)/r^5] + g_1\beta HS_1 + g_2\beta HS_2$ which incorporates isotropic, anisotropic, and asymmetric exchange, dipole–dipole, and Zeeman terms. The best-fit parameters are r(Fe–Cu distance) = 5 Å, d = 0.01 cm^{-1}, J = +0.25 cm^{-1}, J^{zz} = 0.006 cm^{-1}, K = 0.003 cm^{-1}, g_{Fe} = 3.6, 2.06, 1.19, and g_{Cu} = 2.15, 2.05, 2.05. A comparison is made of the properties of this complex and those of the a_3 sites of the cyanide-treated oxidized forms of bovine and bacterial cytochrome oxidases. While MCD and Mössbauer evidence for the natural oxidases have also indicated an $S' = 1$ ground state, their ESR silence compared to the present model system is explained in terms of the magnitudes of the zero-field splitting terms. The solvent-dependent properties of this complex are described. Solutions in 10% MeOH–$CHCl_3$, with and without 1 mol of 1-methylimidazole, show properties similar to the solid state. In CH_3CN and Me_2SO, little or no exchange coupling is evident, while in DMF an ESR silent species is formed. Possible structures consistent with these observations are presented.

An unequivocal description of the active site of cytochrome *c* oxidase still remains elusive despite the persistent attentions of many research groups who have probed the enzyme with a wide variety of sophisticated and modern techniques.[2] Four redox-active centers, cytochrome *a*,cytochrome a_3, Cu_a, and Cu_{a3} accept four electrons in the terminal stages of the respiratory chain and reduce oxygen to water. From the vast amount of available evidence the following picture, which appears to have general agreement, has emerged. In the oxidized resting state of the enzyme cytochrome *a*, which is low-spin Fe(III), and one of the Cu(II) ions Cu_a are both ESR detectable. The remaining high-spin cytochrome a_3 and Cu_{a3} are ESR silent, and on the basis of magnetic susceptibility[3,4] and MCD[4,5] results, it is generally believed that these are antiferromagnetically coupled to yield an $S' = 2$ spin state ($J > -200$ cm^{-1}). Reduction of oxygen is thought to occur at this center, as other external ligands such as CO, N_3^-, CN^-, NO, and S^{2-} are known to bind only to heme a_3 (and perhaps to Cu_{a3}). Indeed, the CN^--treated oxidized form of the enzyme has been well studied; the iron of heme a_3 is now forced low spin, but both it and the Cu_{a3} remain ESR undetectable.

Bulk magnetic susceptibility measurements of this form have been interpreted in terms of an antiferromagnetically coupled $S' = 0$ ground state with coupling constant $2J \leq -40$ cm^{-1}.[4] However, more recent MCD measurements[6] over the temperature range 1.5–200 K are totally at variance with this model and are consistent with strong ferromagnetic coupling between heme a_3–CN and $-Cu_{a3}$, leading to an $S' = 1$ ground state. This is further split by zero-field splitting leaving an $M_S = \pm 1$ ground state separated by >10 cm^{-1} from the $M_s = 0$ level. The lack of ESR signals is accounted for by forbidden $\Delta M_s = 2$ transitions within the $M_s = \pm 1$ levels. These results have been supported by a Mössbauer study[7] of an ^{57}Fe-enriched bacterial cytochrome oxidase from *Thermus thermophilus* which has been shown to have similar ESR and optical properties to the previously studied bovine enzyme. Low-temperature measurements in applied magnetic fields of the CN^--oxidized form of this enzyme indicate a paramagnetic ground state, again suggesting ferromagnetic coupling resulting in an $S' = 1$ system.

(1) (a) Australian National University; present address: Department of Chemistry, University of New England, Armidale 2351, Australia. (b) Monash University.

(2) For more recent reviews, see: (a) "Cytochrome Oxidase"; King, T. E., Orii, Y., Chance, B., Okunuki, K., Eds.; Elsevier: New York, 1979. (b) Malmstrom, B. G. "Metal Ion Activation of Dioxygen"; Spiro, T. G., Ed.; Wiley: New York, 1980; Chapter 5, p 181. (c) Brunori, M.; Antonini, E.; Wilson, M. T. "Metal Ions in Biological Systems"; Sigel, H., Ed.; Marcel Dekker: New York, 1981; Chapter 6, p 187. (d) Blair, D. F.; Martin, C. T.; Gelles, J.; Wang, H.; Brudvig, G. W.; Stevens, T. H.; Chan, S. I. *Chemica Scripta* **1983**, *21*, 43.

(3) Tweedle, M. F.; Wilson, L. J.; Garcia-Iniguez, L.; Babcock, G. T.; Palmer, G. *J. Biol. Chem.* **1978**, *253*, 8065.

(4) Palmer, G.; Antalis, T.; Babcock, G. T.; Garcia-Iniguez, L.; Tweedle, M.; Wilson, L. J.; Vickery, L. E. "Developments in Biochemistry"; Singer, T. P., Ondarza, R. N., Eds.; Elsevier-North Holland: New York, 1978; Vol. 1, p 221.

(5) Babcock, G. T.; Vickery, L. E.; Palmer, G. *J. Biol. Chem.* **1976**, *251*, 7901.

(6) Thomson, A. J.; Johnson, M. K.; Greenwood, C.; Gooding, P. E. *Biochem. J.* **1981**, *193*, 687.

(7) Kent, T. A.; Münck, E.; Dunham, W. R.; Filter, W. F.; Findling, K. L.; Yoshida, T.; Fee, J. A. *J. Biol. Chem.* **1982**, *257*, 12489.

0002-7863/84/1506-4227$01.50/0

The synthesis of model systems containing binuclear metal centers has been the approach adopted by several groups, including our own, to examine the feasibility of some of the suggested structures for the heme a_3–Cu_{a3} active site.[8-13] This work is beginning to reveal some of the structural requirements for an antiferromagnetically coupled Fe^{III}–Cu^{II} center postulated for the fully oxidized or resting state of the enzyme, although the full structural characterization of a strongly coupled complex has yet to be achieved. The Fe^{III}/Cu^{II} heterobinuclear complexes of our initial ligand system, $\alpha,\alpha,\alpha,\alpha$-tetrakis(*o*-nicotinamidophenyl)-porphyrin, designated $Fe(P)XCu(N_4)^{2+}$, where X = Cl, Br, N_3, and OH have been shown[8a,14,15] to lack significant magnetic coupling between the two metal ions and thus have limited applicability as models for the fully oxidized or resting state of the enzyme. An alternative system which we rationalized in terms of orbital overlap might overcome the deficiencies of the previous ligand, viz., (P)–(NS_2), which has a tridentate ligand strapped perpendicularly across the face of a porphyrin, has involved added complications of the Fe in the porphyrin adopting an intermediate spin configuration;[8b] the solution properties of one complex of this system have indicated magnetic coupling, although a crystal structure still eludes us.

Nevertheless, the CN^--bridged complex of our $Fe(P)XCu(N_4)^{2+}$ system has now been studied in detail, and we find that the solvent-dependent properties display ferromagnetic, antiferromagnetic, and uncoupled behavior within the same basic ligand system. As such, it allows the basis for a distinction to be made as to the possible mode of coupling in the CN^- oxidized form of cytochrome oxidase itself.

Experimental Section

Synthesis. A solution of $Fe(P)Cl(N_4)\cdot CHCl_3$[16] (620 mg, 0.475 mmol) in $CHCl_3$ (200 mL) was washed successively with 5% aqueous NaOH (2 × 200 mL), H_2O (200 mL), and 5% aqueous NaCN (200 mL) acidified with 0.05 M H_2SO_4 (50 mL) (×3) and H_2O (200 mL). The deep red solution was dried over Na_2SO_4, evaporated to dryness at <20 °C, immediately redissolved in $CHCl_3$ containing 10% MeOH (200 mL), and treated with a solution of $Cu(ClO_4)_2\cdot xH_2O$ in MeOH (0.1 M in Cu^{2+}, 4.85 mL, 0.485 mmol). After 15 min at room temperature, the solution was evaporated to dryness, and the residue was recrystallized by slow addition of water to an acetonitrile solution at <30 °C to yield a purple microcrystalline solid. A second recrystallization by diffusion of pentane into a $CHCl_3$–MeOH solution gave brown-red plates (0.50 g, 70%) of the *trihydrate* $[Fe(P)CNCu(N_4)](ClO_4)_2\cdot 3H_2O$ (**1**). Anal. Calcd for $C_{69}H_{44}N_{13}O_{12}FeCuCl_2\cdot 3H_2O$: C, 55.57; H, 3.38; N, 12.20; Fe, 3.74; Cu, 4.26. Found: C, 55.25; H, 3.35; N, 12.12; Fe, 4.29; Cu, 4.18.

Physical Measurements. Magnetic susceptibility data, ESR spectra, Mössbauer spectra and UV–vis spectra were collected as previously described.[16]

Results and Discussion

Synthesis. *meso*-$\alpha,\alpha,\alpha,\alpha$-tetrakis(*o*-nicotinamidophenyl)-porphyrin (P)–(N_4) and the chloro Fe(III) complex $Fe(P)Cl(N_4)\cdot CHCl_3$ were synthesized as previously described with due precautions to ensure the presence of only a single atropisomer in the final product.[16] Conversions to the CN^- complex via the hydroxo compound and thence to the binuclear Fe/Cu complex were performed under mild conditions without isolation of the intermediates. Recrystallizations were performed at room temperature to avoid possible isomerization. A solution of the mononuclear CN^- complex $Fe(P)CN(N_4)$, required for ESR measurements (see below), was also prepared in situ in a similar manner. Such solutions, in the absence of excess CN^-, were somewhat unstable in the presence of hydroxylic solvents and decomposed slowly over several hours at room temperature. The Fe/Cu complex, on the other hand, appears indefinitely stable in both solution and the solid state. Although the complex is highly crystalline, we have not yet been successful in obtaining single crystals of X-ray diffraction quality. By analogy with the corresponding chloro complex $[Fe(P)ClCu(N_4)](ClO_4)_2$, which has been shown by X-ray analysis[8a] to have an intramolecular bridging Cl^- ion, we propose structure **1** (Figure 1) for the present complex. The fact that the CN^- is bridging the Fe(III) and Cu(II) is evident from the magnetic properties (see below); we are, however, unable to distinguish between the monomeric structure **1** and a polymeric structure with the CN^- outside the "pocket", bridging Fe(III) and Cu(II) ions intermolecularly. Nevertheless this does not affect the following discussion, as the overall interaction is similar in both cases.

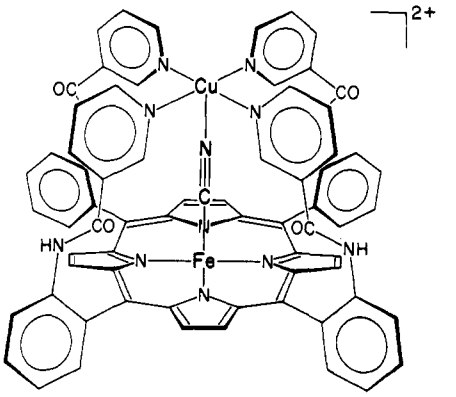

Figure 1. Proposed structure of $[Fe(P)CNCu(N_4)]^{2+}$ cation of **1**. Water molecules possibly occupying the sixth coordination sites at Fe and Cu are not shown.

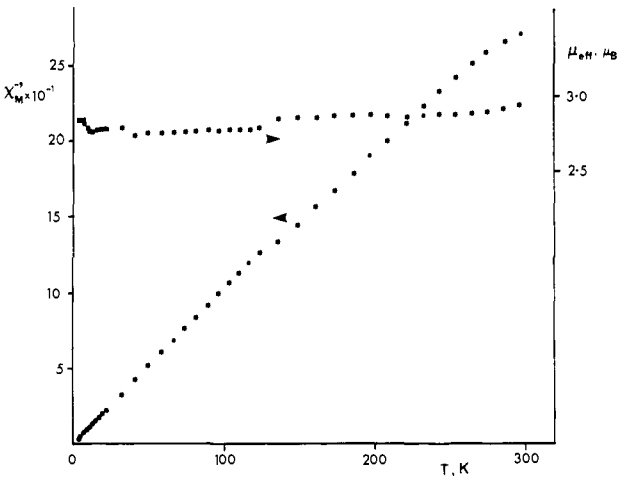

Figure 2. Temperature dependence of the magnetic moments (μ_{eff}) and reciprocal susceptibility (χ^{-1}) of **1**. The slight discontinuity in the experimental data at 123 K is of instrumental origin.

Magnetic Susceptibility. Plots of the magnetic moments and reciprocal susceptibilities of $[Fe(P)CNCu(N_4)](ClO_4)_2\cdot 3H_2O$ (**1**) as a function of temperature (300–4.2 K) are shown in Figure 2. Tabulated data are given as supplementary material. The magnetic moment is essentially temperature independent and varies between 2.84 μ_B (per molecule) at 4.3 K and 2.95 μ_B at 295 K. There is a small but significant increase below 10 K. The reciprocal susceptibilities display a linear Curie–Weiss dependence

(8) (a) Gunter, M. J.; Mander, L. N.; McLaughlin, G. M.; Murray, K. S.; Berry, K. J.; Clark, P. E.; Buckingham, D. A. *J. Am. Chem. Soc.* **1980**, *102*, 1470. (b) Gunter, M. J.; Mander, L. N.; Murray, K. S.; Clark, P. E. *Ibid.* **1981**, *103*, 6784.

(9) Petty, R. H.; Welch, B. R.; Wilson, L. J.; Bottomley, L. A.; Kadish, K. M. *J. Am. Chem. Soc.* **1980**, *102*, 611. Dessens, S. E.; Merrill, C. L.; Saxton, R. J.; Ilaria, R. L., Jr.; Lindsay, J. W.; Wilson, L. J. *Ibid.* **1982**, *104*, 4357. Saxton, R. J.; Olson, L. W.; Wilson, L. J. *J. Chem. Soc., Chem. Commun.* **1982**, 984.

(10) Eliot, C. M.; Akabori, K. *J. Am. Chem. Soc.* **1982**, *104*, 2671.

(11) Chang, C. K.; Koo, M. S.; Ward, B. *J. Chem. Soc., Chem. Commun.* **1982**, 716.

(12) Landrum, J. T.; Grimmett, D.; Haller, K. J.; Scheidt, W. R.; Reed, C. A. *J. Am. Chem. Soc.* **1981**, *103*, 2640.

(13) Okamato, M.; Nishida, Y.; Kida, S. *Chem. Lett.* **1982**, 1773. Okawa, H.; Kanda, W.; Kida, S. *Ibid.* **1980**, 1281.

(14) Berry, K. J.; Clark, P. E.; Gunter, M. J.; Murray, K. S. *Nouv. J. Chim.* **1980**, *4*, 581.

(15) Gunter, M. J.; Berry, K. J.; Murray, K. S.; Clark, P. E., unpublished results.

(16) Gunter, M. J.; McLaughlin, G. M.; Berry, K. J.; Murray, K. S.; Irving, M.; Clark, P. E. *Inorg. Chem.* **1984**, *23*, 283.

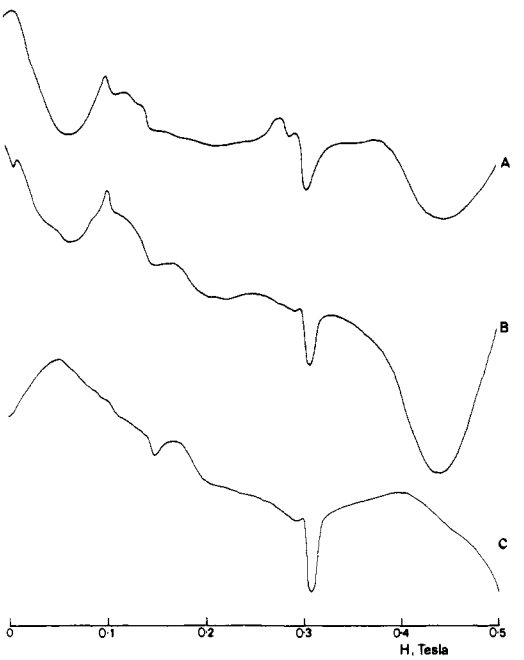

Figure 3. X-band ESR spectra at 4.2 K of **1**: (A) Solid state (powder), (B) 10% MeOH–$CHCl_3$ solution, (C) 10% MeOH–$CHCl_3$ solution containing 1 mol of 1-methylimidazole.

on temperature, except for a small deviation at temperatures above ca. 260 K. In a preliminary communication we noted that the μ vs. T plot for **1** was quite different to that of the chloro-bridged complex $[Fe(P)ClCu(N_4)](ClO_4)_2$, and was compatible with a low-spin Fe(III) center.[14] The nature and extent of intramolecular coupling between the Fe and Cu centers, which were not pursued in detail at that time, are described below.

ESR Spectra. The X-band ESR spectrum of a powdered sample of the complex **1** measured at 4.2 K is shown in Figure 3A. The lines broaden and disappear as the temperature is raised to 30 K. The line shape is unusual and complex and is reproducible between samples. Intense broad lines occur below 1500 G and above 4000 G. Poorly resolved lines are observed at "g" ca. 2, which is where monomeric Cu(II) and low-spin Fe(III) porphyrin lines are expected, but the line shape is atypical of either. A weak narrower line is seen at g 6 and a broad ill-resolved line at g ca. 3.8. A sloping base line sweeps from top left to bottom right. Because of the broad nature of the spectrum, and the difficulty in deciding whether a peak crosses the base line or not, the g values given are only an approximate description of the field–frequency relationship of the spectral lines and are not meant to be taken as the true g tensors of the Zeeman terms in the spin Hamiltonian. The broadness of the lines presumably arises from a combination of dipolar and exchange broadening.

In order to obtain the g values for the iron center alone, i.e., without the Cu(II) ion present, the complex $[Fe(P)CN(N_4)]$ was created in situ by adding HCN to a dichloromethane solution of $[Fe(P)OH(N_4)]$.[16] The spectrum gives lines at g = 3.6, 2.06, and 1.19, which are assigned to the mono-cyano species by analogy with other monocyano heme spectra. A small g 6 line is assigned to residual $Fe(P)OH(N_4)$ and a g 2.51 line to some dicyano adduct that is also formed.

Mössbauer Spectra. Mössbauer spectra of a polycrystalline sample of **1** obtained at the three temperatures 300, 77, and 4.2 K each show a single sharp doublet indicating the existence of a unique coordination for the iron atom (Figure 4). The isomer shifts δ, quadrupole splittings ΔE, full widths at half-maximum height of each line of the doublet, and intensity ratio of the two lines are given in Table I. These values are typical of low-spin iron(III) porphyrin complexes.[17]

(17) Sams, J. R.; Tsin, T. B. In "The Porphyrins"; Dolphin, D., Ed.; Academic Press: New York, 1979; Vol. IV, Chapter 9, p 425.

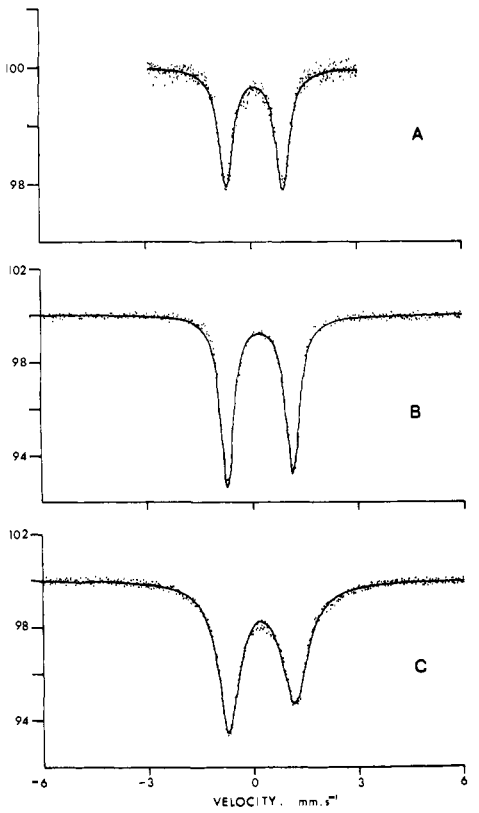

Figure 4. Zero-field Mössbauer spectrum of **1** at various temperatures: (A) 300 K, (B) 77 K, (C) 4.2 K. The solid lines are the fits using the parameters given in Table I.

Table I. Mössbauer Parameters for **1** in Zero Applied Field

temp, K	δ (±0.01), mm s^{-1} [a]	ΔE (±0.01), mm s^{-1}	fwhm (±0.01), mm s^{-1} [b]	intensity[c] ratio
300	0.145	1.60	0.24, 0.24	1.00
77	0.23	1.86	0.22, 0.23	0.92
4.2	0.24	1.87	0.36, 0.45	0.81

[a] With respect to α-Fe at room temperature. [b] Full width at half-maximum height of each line. [c] Intensity ratio of two lines of the doublet.

At room temperature the two lines of the doublet have the same intensity, indicating that the electronic spin–lattice relaxation time is much shorter than the nuclear Larmor precession time ($\sim 10^{-7}$ s). As the temperature is lowered the relative intensity of the higher energy line decreases and the line becomes broader, but with the areas under the two lines remaining equal. This behavior is common in systems in which the spin–lattice relaxation rate decreases with decreasing temperature. Since the higher energy line broadens preferentially, this suggests that the axial component of the electric field gradient, V_{zz}, must be positive. Mössbauer spectra obtained in an applied magnetic field confirm this assignment, so that the ground state for this complex is the orbital singlet $(d_{xy})^2(d_{xz}d_{yz})^3$.

The temperature dependence of the isomer shift is entirely due to the second-order Doppler shift. The decrease in the quadrupole splitting between 77 and 300 K indicates that at higher temperatures thermal electronic population of the low-lying orbitals is becoming significant, so that the quadrupole interaction must be calculated as a thermal average over these occupied doublets.

Mössbauer spectra were obtained at 4.2 K in magnetic fields of 1.25 and 25 kOe applied parallel to the direction of γ-ray propagation. The effect of the smaller applied field was to cause some diffuse broadening in the wings of the spectrum. In the larger field the spectrum displayed large hyperfine splitting, confirming the paramagnetic nature of the iron, but the features of the spectrum were not well defined (Figure 5).

Data Analysis. Ignoring for the moment the ESR and Mössbauer data, it is possible to fit the magnetic susceptibility

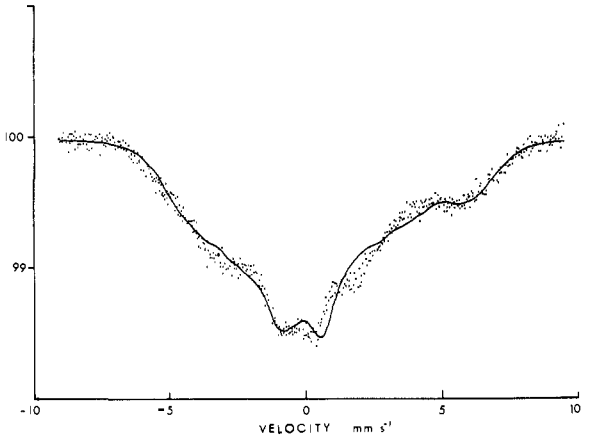

Figure 5. Mössbauer spectra of **1** at 4.2 K in a 25 kOe magnetic field applied parallel to the direction of γ-ray propagation. The solid line is the fit using the parameters given in Table IV for anisotropic g, as described in the text. The fit using the isotropic g values of Table IV was of similar quality.

Table II. Spin Hamiltonian Used To Calculate ESR Spectrum and Magnetic Susceptibilities of Coupled $S_1 = {}^1/_2$ and $S_2 = {}^1/_2$ Ions in **1**

$\mathcal{H}$	
$-JS_1S_2$	isotropic exchange
$+J_D^{\alpha\beta}/[2\{S_1^{\alpha}S_2^{\beta} + S_1^{\beta}S_2^{\alpha}\}]$	anisotropic exchange
$+d(S_1 x S_2)$	asymmetric exchange
$(+\mu_1\mu_2/r^3) - [3(\mu_1 r)(\mu_2 r)/r^5]$	direct dipole–dipole
$+g_1\beta HS_1 + g_2\beta HS_2$	Zeeman

data to two different models, both of which give $S' = 1$ ground states. First, if strong antiferromagnetic coupling between intermediate-spin iron ($S_{Fe} = {}^3/_2$) and copper ($S_{Cu} = {}^1/_2$) is assumed then a good fit to the data is obtained at all temperatures except for the small observed increase in $\bar{\mu}$ at very low temperatures, the J value being 188 cm^{-1} (i.e., quintet–triplet splitting of 750 cm^{-1}). A ${}^3/_2$ spin state on Fe might be expected to lead to a rapid decrease in $\bar{\mu}$ below ca. 20 K on account of zero-field splitting effects. This is not observed. The second model employs a $S_{Fe} = {}^1/_2$ state for iron, which is perhaps intuitively more reasonable for monocyanoiron porphyrins[18] and for which no decrease in $\bar{\mu}$ due to ZFS effects would be expected at low temperatures. The Mössbauer spectral analysis (vide infra) confirms the low-spin nature of the Fe center. A reasonable fit of the susceptibility data can be obtained by adding together typical χ_{Fe} and χ_{Cu} values to *uncoupled* iron and copper components and assuming Curie behavior for each. However, the ESR spectrum of powder samples of **1** at 4.2 K (Figure 3A) clearly does not correspond to a superposition of $S_{Fe} = {}^1/_2$ iron porphyrin and $S = {}^1/_2$ copper pyridinate resonances, where one might expect to see lines at $g \sim 3$, 2.5, and 1.5 and 2.2 (with hyperfine splitting) and 2.05, due to Fe and Cu, respectively.

The ESR spectrum is in fact reminiscent of triplet-state ($S' = 1$) spectra arising from coupled $S = {}^1/_2$ pairs.[19,20] These are well-known for Cu–Cu systems, but not for Fe–Cu.

Since lines are observed at 4.2 K, they presumably arise through population of ground-triplet-state levels, the latter being formed either by ferromagnetic exchange coupling or by dipole–dipole coupling (with very weak exchange). In order to try to fit simultaneously the susceptibility and ESR results, we have made calculations using the spin Hamiltonian shown in Table II, which incorporates isotropic, anisotropic, and asymmetric exchange as well as direct dipole–dipole terms. These terms are likely to be important in heterobinuclear systems where each of the component metal ions possess different symmetry and different magnetic tensors.[21] In homobinuclear systems, e.g., Cu^{II}–Cu^{II}, it is generally possible to use a more restricted Hamiltonian. We deliberately included all of the terms shown in Table II, since it provided a convenient way of focussing on the effects of different contributions to the overall interaction.

The anisotropic exchange term in its general form (i.e., nine components of $\alpha\beta$) would incorporate the isotropic, asymmetric, and dipolar parts, but it was desirable to separate out these interactions. The theoretical derivation used here is based on the work of Erdos,[22] which has been reviewed by Kokoszka[21] and Ginsberg.[23] Allowance was made in the calculations to allow for a reorientation of the coordinates on the magnetic centers to suit the present geometry. The z component of the anisotropic exchange, J^{zz}, lies along the Cu–Fe direction, while the x–y anisotropy is represented by a parameter K. Kokoszka[21] and Ginsberg[23] have both given clear descriptions of the effects of anisotropic and asymmetric exchange on the energy levels of a pair of spin ${}^1/_2$ ions although neither explicitly separated out the effect of dipolar coupling, and so this contribution remains absorbed in the other terms. Before discussing our attempts to fit the present data, we give a brief summary of the points discussed by these authors. Both J^{zz} and d give rise to zero-field splitting of the triplet state into a doublet and a singlet with separations of $3J^{zz}/4$ (for $d = 0$) and $\simeq d^2/16J$ (for $J^{zz} = K = 0$), respectively. Depending on the relative signs of these two interactions, their combined effects may be to augment or cancel out the resulting zero-field splitting. The x–y anisotropy, K, further splits the $M_s \pm 1$ doublet by energy $2K$ in zero field. The magnitudes of J^{zz} and d are approximately $(\Delta g/g)^2 J$ and $(\Delta g/g)J$, respectively, where $\Delta g = |g - 2|$.[22] In a situation of the present type, with anisotropic g tensors on both the Fe^{III} and Cu^{II} ions, the differences in the g values will therefore sensitively perturb the energy levels. The general order of magnitude of the interactions is expected to be $J >> d > J^{zz}$, although there are few experimental data available to test this ordering. Ginsberg[23] has pointed out that susceptibility measurements are only capable of detecting anisotropic exchange in the ~4 K region of ferromagnetically coupled pairs and not capable of detecting anisotropic exchange in antiferromagnetically coupled pairs. ESR measurements should, however, be a much more sensitive probe for such interactions.

The dipole–dipole term in Table II, either alone or in the presence of weak isotropic exchange, has been applied extensively by Pilbrow and Smith to the ESR spectra of similar or dissimilar $S = {}^1/_2$ ion pairs.[19,24] Dipolar coupling dominates the zero-field splitting of the spin triplet levels when J is small in size and leaves the $M_s \pm 1$ levels lowest in energy. Interestingly, Palmer[25] has recently used the DISYMM program of Pilbrow[24] to simulate the ESR spectrum of Fe^{III}(heme a)/Cu^{II}(detectable) pairs in cytochrome oxidase assuming dipolar coupling between the ions when separated 5 Å. Since the r, g_{Fe}, and g_{Cu} values used by Palmer were very similar to those observed in the present compound, reproduction of the line positions given[25] in Palmer's review (see his Figure 11.2), provided a useful test of the correctness of the present calculations.

By use of the computer diagonalization of the complete Hamiltonian given in Table II, a set of energy levels was obtained for each of the principal directions as a function of magnetic field. The positions at which possible resonances would occur could then be ascertained in the usual way by incorporating the X-band quantum of energy, $h\nu$. The various exchange and dipolar-coupling contributions could be turned on and off in turn to observe their

(18) Monocyanoiron(III) porphyrins have only recently been structurally characterized. Scheidt, W. R.; Lee, Y. J.; Luangdilok, W.; Haller, K. J.; Anzai, K.; Hatano, K. *Inorg. Chem.*, **1983**, *22*, 1516. Crystals of [Fe(TPP)CN(py)]H_2O and earlier studies of monocyano species in solution show $S = {}^1/_2$ Fe behavior.

(19) Smith, T. D.; Pilbrow, J. R. *Coord. Chem. Rev.* **1974**, *13*, 173.

(20) Gatteschi, D. In "ESR and NMR of Paramagnetic Species in Biological and Related Systems"; Bertini, I., Drago, R. S., Eds.; D. Reidel: Holland, 1979; p 255.

(21) Kokoszka, G. F.; Gordon, G. In "Transition Metal Chemistry"; Carlin, R. L., Ed.; Marcel Dekker: New York, 1969; Vol. 5, p 181. Kokoszka, G. F., Duerst, R. W. *Coord. Chem. Rev.* **1970**, *5*, 209.

(22) Erdos, P. *J. Phys. Chem. Solids* **1966**, *27*, 1705.

(23) Ginsberg, A. P. *Inorg. Chim. Acta Rev.* **1971**, *5*, 45.

(24) Boas, J. F.; Hicks, P. R.; Pilbrow, J. R.; Smith, T. D. *J. Chem. Soc. Faraday Trans. 2* **1978**, *74*, 417.

(25) Palmer, G. *Adv. Inorg. Biochem.* **1980**, *2*, 153.

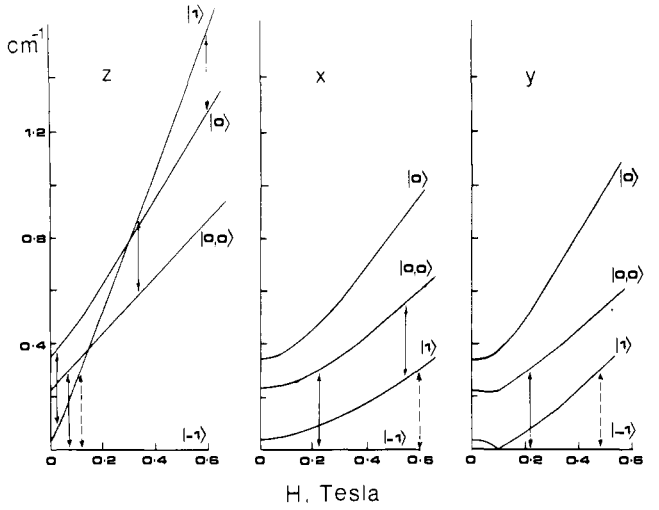

Figure 6. Energy level diagrams for the x, y, and z directions as a function of magnetic field for **1** assuming *only* dipole–dipole coupling between Fe and Cu. r was set at 5 Å, and the g values were those given in Table III. The solid vertical arrows represent allowed $\Delta M_s = 1$ transitions at X-band frequency, while the dashed arrows represent forbidden $\Delta M_s = 2$ transitions.

separate or combined effect on the energy levels. Some reasonable assumptions were made in order to minimize the number of variable parameters. Thus g_{Fe} and g_{Cu} were fixed at the values observed for Fe(P)CN(N_4) and anticipated for a copper pyridinate complex. The Cu–Fe distance, r, was fixed at 5 Å, which is compatible with the ligand geometry[16] and is the value observed in a related cyano-bridged dimer of known crystal structure.[26] Furthermore, the calculated energy levels were very sensitive to small variations in r, and it was found that 5 ± 0.1 Å gave the best fit. The anisotropic exchange parameter K was set at $0.5J^{zz}$, while the asymmetric exchange parameter d was assumed to be isotropic.[21-23]

The main features of the powder ESR spectrum that had to be reproduced were the strong broad lines at low and high field, viz.: ~1000 and ~4500 G (Figure 3A). Since our computer program also yields μ as a function of temperature it was possible to use the observed magnetic moment data, particularly the small increase in μ at very low temperature, as a check on the choice of parameters. Variations in the size and sign of the isotropic exchange contribution directly affect the magnetic moments, and a value of J of less than ca. +0.5 cm^{-1} was found to be compatible with the μ/T data. This small value seems reasonable in view of the length of the Cu–Fe distance and in relation to J values observed in other cyano-bridged Cu–Cu species,[27] although in principle it is possible to get stronger coupling over such distances.[23,28]

Calculations using J equal to zero or to small negative values did not fit either the μ/T data or the ESR line positions. The energy levels for a purely dipolar interaction are shown in Figure 6, and it can be seen that the resonance positions do not correspond to those observed. Futher, the μ values were calculated to vary from 2.82 μ_B at 30 K to 2.84 μ_B at 4 K, which is a smaller increment in this temperature interval than the observed increment of 0.06 μ_B, i.e., 2.78 μ_B at 30 K; 2.84 μ_B at 4.3 K. (Use of a small negative value of J of −0.25 cm^{-1} leads to a calculated μ value of 2.81 μ_B, which remains independent of temperature between 30 and 4.3 K.)

The best correspondence between calculated and observed ESR line positions was for J ca. +0.25 cm^{-1}. The main effect of variation in J is on the energies of the singlet, $|0, 0\rangle$, levels relative to the triplet levels. $\Delta M_s = 1$ lines are predicted at ca. 1000 and

(26) Roder, P.; Ludi, A.; Chapuis, G.; Schenk, K. J.; Schwarzenbach, D. *Inorg. Chim. Acta* **1979**, *34*, 113.
(27) Bieksa, D. B.; Hendrickson, D. N. *Inorg. Chem.* **1977**, *16*, 924.
(28) Coffmann, R. E., Buettner, G. R. *J. Phys. Chem.* **1979**, *83*, 2387; 2392.

Table III. Best-Fit Parameters to ESR and μ_{eff}/T Data for **1**

r(Cu–Fe distance) = 5 Å	g_{Fe} = 3.6, 2.06, 1.19[a]
J = +0.25 cm^{-1}	g_{Cu} = 2.15, 2.05, 2.05[a]
J^{zz} = 0.006 cm^{-1}, K = 0.003 cm^{-1}, d = 0.01 cm^{-1}	

[a] These values were constrained to the observed single-ion values.

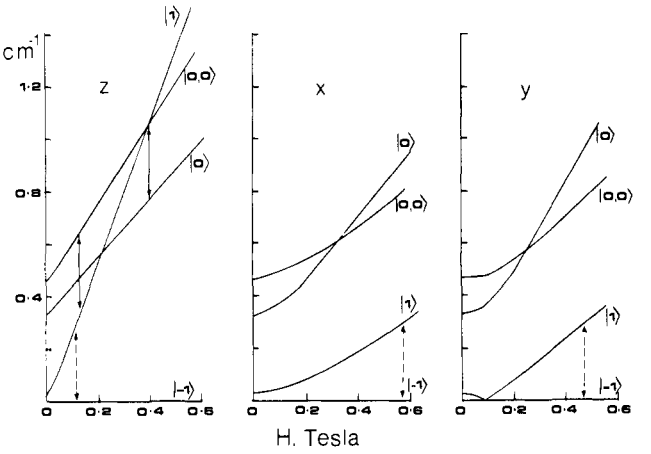

Figure 7. Energy level diagrams for the x, y, and z directions as a function of magnetic field for **1**, calculated by using the Hamiltonian given in Table II with the parameter values given in Table III. The energies are given relative to those of the $|1, -1\rangle$ levels, which are set at zero. The solid vertical arrows represent allowed ESR transitions at X-band frequency, while the dashed arrows represent forbidden ΔM_s = 2 transitions.

4000 G in the z direction when using J of +0.25 cm^{-1}, together with $\Delta M_s = 2$ lines at ca. 1000 (z), 4700 (y), and 5800 G (x). Smaller values of J move the low-field lines toward zero field but also move the 4000-G line downfield. A slightly larger value of J, such as +0.5 cm^{-1}, eliminates the low-field line and predicts two high-field $\Delta M_s = 1$ lines at ca. 3300 (z) and 4250 G (z), with the forbidden lines in similar positions to those described above for J of +0.25 cm^{-1}. For J of +0.5 cm^{-1} the values of μ vary from 2.82 μ_B at 30 K to 2.89 μ_B at 4 K.

The values of the anisotropic and asymmetric parameters used in the calculations were chosen in relation to the size of J as described by Erdos.[22] Thus for J = +0.25 cm^{-1} starter values were d = 0.01 cm^{-1}, J^{zz} 0.006 cm^{-1}, and K = 0.003 cm^{-1}. It was found that variations around these very small values had very little effect on the energy levels. Increase in J^{zz} and K led to small decreases in the energies of the $|0, 0\rangle$, $|1, 0\rangle$, and $|1, 1\rangle$ levels relative to the ground $|1, -1\rangle$ level but did not significantly affect the predicted line positions.

The parameters that best fit the ESR spectrum and magnetic data are given in Table III, the corresponding energy levels being shown in Figure 7. The triplet ground state is split in zero field by ca. 0.32 cm^{-1}, and a small splitting of the $|1, 1\rangle$ and $|1, -1\rangle$ levels of ca. 0.025 cm^{-1} is evident. The $|0, 0\rangle$ level lies 0.47 cm^{-1} above the $|1, -1\rangle$ ground level. The chief contributions to this zero-field splitting are the dipole–dipole coupling followed by the isotropic exchange coupling with a minor effect from the anisotropic terms.

It is also possible to fit the ESR line positions by assuming an isolated triplet ground state, i.e., very strong isotropic ferromagnetic coupling. Under these conditions the anisotropic and asymmetric exchange terms primarily cause zero-field splitting of the triplet state. However, the calculated magnetic moments, especially at low temperatures, are much larger than those observed and agreement between them can only be achieved by reducing the g_{Fe} values below acceptable limits. The set of parameters that best fit the ESR line positions and the magnetic moments under these conditions are as follows: r = 5.0 Å; J = +600 cm^{-1}; J^{zz} = 0.25 cm^{-1}; g_{Fe} = 2.95, 2.03, 0.95; g_{Cu} = 2.15, 2.05, 2.05. These g values for Fe are inconsistent with typical heme cyanides (sum of the squares of the g tensors $\ll 16$ rather than ≥ 16[29]), and are

Table IV. g and A Tensors for Computer Fits of the Mössbauer Spectrum of **1** in an Applied Field of 25 kOe

	g isotropic	g aniso-tropic		g isotropic	g aniso-tropic
g_x	2.0	1.18	A_x[a]	+0.46	+2.51
g_y	2.0	2.26	A_y	+0.32	+0.12
g_z	2.0	1.21	A_z	+5.35	+5.57

[a] mm s^{-1}.

considerably different from the g values of the mononuclear complex Fe(P)CN(N_4), the cyanide form of cytochrome oxidase itself ($g_z \simeq 3.6$), and of other low-spin heme–CN^- complexes.[29] In view of this and the reasons given earlier, it seems more likely that weak ferromagnetic exchange is occurring in the present compound.

In the general context of dissimilar-ion magnetic interactions, we note that other theoretical approaches could have been employed in an attempt to explain the ESR spectrum of the kind shown in Figure 3A. A spin Hamiltonian incorporating axial (D) and rhombic (E) zero-field splitting parameters, pioneered by Bleaney and Bowers,[30] has commonly been used to interpret spin triplet spectra of the kinds observed in distorted Ni(II) monomers[31] or in Cu^{II}–Cu^{II} dimers.[19-21] This approach suffers in comparison to the present one in that it focusses chiefly on the (coupled) triplet state, using average g values and consequently loses its input from the individual metal ions; it is therefore more appropriate to large J situations. The axial splitting D is made up of contributions from anisotropic, asymmetric, and dipolar terms as described above.[32]

Recent work by Gatteschi et al.[33,34] on various mixed-metal dimers has remedied this situation somewhat by using more complete spin Hamiltonians that incorporate anisotropic and asymmetric exchange components as well as individual g values. The parameters used by Gatteschi et al. are different to those used here, and while they are related to or contained within the present ones, they do not follow simple and obvious relationships.

Turning finally to the analysis of the Mössbauer results, attempts were made to least-squares fit the high applied field spectrum on the assumption that the iron was in a pure $S = {}^1/_2$ state. A version of the fitting program described by Lang and Dale[35] was used. The program employs a series of parameters, including the principal components of the electronic g tensor and the magnetic hyperfine A tensor and the quadrupole interaction, which may be varied to describe the data. Various constraints can be applied, and spectra from powdered samples are accommodated by summing the contributions for many orientations of the principal tensor axes (assumed the same for g and A) relative to the γ-ray direction.

The g and A tensors were each allowed to vary, both isotropically and anisotropically. Reasonable fits could only be obtained using an anisotropic A tensor in which A_z was large and positive. However, there was no difference in the quality of the fit when g was taken as isotropic, $g = 2$, or allowed to vary anisotropically. The values for g and A in these two cases are shown in Table IV, those in the anisotropic case being markedly different to the g values observed for Fe(P)CN(N_4). The spectrum may be simply understood in terms of an isotropic g and a single component, A_z, as has been demonstrated by Lang and Oosterhuis.[36] For isotropic g all directions of the effective electronic spin must be considered with equal weight, and the strongly axial A tensor ensures that the nucleus sees an internal field proportional to cos θ, averaged with equal weights over all directions in space. Thus all fields from zero to the maximum will be present, and the spectrum will be smeared out.

An alterantive explanation for the broad line shape in applied field is that mentioned briefly by Münck et al.[7] to explain the cyanide-oxidized cytochrome oxidase spectrum, viz., induced hyperfine interactions arising from ferromagnetic coupling to the Cu(II) ion. This could explain the poor agreement between the observed line shape and that calculated by the Lang and Dale program using the single-ion Fe(P)CN(N_4) anisotropic g values. Some intercluster coupling may also contribute to the broadened line shape.

Solution Behavior. Although we can rationalize the solid-state properties of this compound in terms of a weak ferromagnetic coupling, we have found a complex and varied solvent-dependent behavior in solution. Details of the visible spectra, IR C≡N absorption, magnetic moment at 300 K, and ESR features of [Fe(P)CNCu(N_4)](ClO_4)$_2$ in various solvents at 4.2 K are collected in Table V. Also included in this table are proposed structures and nature of the magnetic coupling, which is consistent with this and other data. A full discussion now follows.

The similarities in the visible spectra and the C≡N stretching frequency in the IR spectra, which is very weak and difficult to detect in most cases, indicate that the CN^- is bound to the Fe in the porphyrin, enforcing a low-spin state on the metal. Given the well-known affinity for 6-coordination in low-spin cyano hemes in general, it is reasonable to assume a solvent or added ligand trans to the strong-field CN^- ligand in each case;[18] it is to be noted that the visible absorption of the present CN^- complexes are distinct from those of other 6-coordinate hemichromes of this ligand system in the presence of a large excess of added ligand (for example, [Fe(P)(NMeIm)$_2$(N_4)]$^+Cl^-$ has λ_{max} 418, 552, and 635 nm in both Me_2SO and 10% MeOH–$CHCl_3$).[16]

The effective magnetic moment per molecule at 300 K as determined by the Evans NMR method is the same within the limits of the measurements (3.4–3.5 μ_B) in all solvents tested in Table V. As pointed out above in the discussion of the solid-state magnetic properties, such a value can result from the presence of uncoupled low-spin Fe(III) ($S = {}^1/_2$) and Cu(II) ($S = {}^1/_2$) or weakly coupled ions.[37]

The close similarity of the ESR spectrum in 10% MeOH–$CHCl_3$ solution to that of the solid state (Figure 3) implies a near identical magnetic situation in each case, and thus a structure as indicated in Table V is likely: an Fe that is 6-coordinate with methanol and bridging cyanide ligands. We cannot distinguish between a square-pyramidal 5-coordination arrangement around Cu and a tetragonal ligand field involving a second methanol, hence the parentheses around the MeOH at the Cu^{2+} ion. In 10% MeOH–$CHCl_3$ containing 1 mol of 1-methylimidazole, the ESR spectrum is altered somewhat, but the essential features remain the same; the broad absorption at low magnetic fields and the very strong broad absorption around 6000 G (not fully shown in Figure 3C) are shifted slightly from their positions in the same solvent system without added base, which might be expected if the imidazole occupies the sixth coordination site at Fe, leading to an alteration of the g term anisotropies; it is clear from Figure 7 that this would significantly alter the line positions. The overall structural features remain, however, and the magnetic coupling is weakly ferromagnetic in nature. Addition of excess 1-methylimidazole results in the appearance in the ESR of strong signals around $g = 2$ typical of Cu(II) nitrogen base complexes.

(29) Palmer, G. In "The Porphyrins"; Dolphin, D., Ed.; Academic Press: New York, 1979; Vol. IV, Chapter 6, p 313. Griffith, J. S. *Mol. Phys.* **1971**, *21*, 135.

(30) Bleaney, B.; Bowers, K. D. *Proc. R. Soc. London, Ser. A* **1952**, *214*, 451. See also: Abragam, A.; Bleaney, B. In "Electron Paramagnetic Resonance of Transition Ions", Oxford University Press: Oxford, 1970; p 152.

(31) Reedijk, J.; Nieuwenhuijse, B. *Recl. Trav. Chim. Pays-Bas* **1972**, *91*, 533.

(32) For discussions of how exchange and dipolar terms may be related to the spin Hamiltonian parameters D and E, see ref 19, 21 and 28.

(33) Banci, L.; Bencini, A.; Dei, A.; Gatteschi, D. *Inorg. Chem.* **1981**, *20*, 393. Bencini, A.; Gatteschi, D. *Mol. Phys.* **1982**, *47*, 161.

(34) Banci, L.; Bencini, A.; Gatteschi, D. *Inorg. Chem.* **1981**, *20*, 2734.

(35) Lang, G.; Dale, B. W. *Nucl. Instrum. Methods* **1974**, *116*, 567.

(36) Lang, G.; Oosterhuis, W. T. *J. Chem. Phys.* **1969**, *51*, 3608.

(37) The solution moments are a little higher than the solid-state sample. However, low-spin cyano hemes have been shown to have moments in excess of the spin-only value, up to 2.6 μ_B.[18] Such a value, together with a typical Cu(II) moment of 2.0–2.1 μ_B could give rise to moments of the order indicated, in the absence of significant coupling. A high spin ⇌ low spin equilibrium is also possible in solution, giving rise to small high-spin Fe(III) signals in the ESR spectra in some solvents.

Table V. Physical Characteristics, Proposed Structures, and Nature of Magnetic Coupling for **1** in Various Solvents

solvent	vis spectrum λ_{max}, nm	IR $\nu_{C\equiv N}$, cm^{-1}	μ_{eff} at 300 K, μ_B/mol[a]	ESR at 4.2 K (apparent g values)	proposed structures[b]	nature of magnetic coupling[b]
none		2150	2.95	9.3, 5.9, 5.0, 2.3, 2.0, 1.4	$H_2O\overline{FeCNCu}(H_2O)$	ferromagnetic
10% MeOH–$CHCl_3$	419, 537	2143	3.5	9.0, 6.1, 5.5, 3.7, 2.0, 1.4	$MeOH\overline{FeCNCu}(MeOH)$	ferromagnetic
10% MeOH–$CHCl_3$ + 1 mol of 1-MeIm	419, 543, 630 (sh)[c]		3.4	11.9, 3.7, 2.0, 1.1	$MeIm\overline{FeCNCu}(MeOH)$	ferromagnetic
MeCN	418, 537, 635 (sh)	2100, 2140	3.4	3.58, 2.14, 1.38 (Fe) 2.25, 2.05 (Cu)	$NC\overline{FeMeCNCu}MeCN$	none
Me_2SO	419, 543, 625 (sh)	2130	3.5	6.0, 2.0 (1.1) (Fe) 2.24, 2.05 (Cu)	$NC\overline{FeMe_2SOCu}Me_2SO$[d]	none
DMF	420, 541, 626 (sh)	2080, 2120	3.5	ESR silent	$DMF\overline{FeCNCu}DMF$	antiferromagnetic or ferromagnetic

[a] Measured by the Evans NMR method. [b] See text for detailed discussion. The lines enclosing the Fe and Cu represent the (P)–(N_4) ligand system. Polymeric structures are also possible. [c] Concentration dependent; these figures are for a 1 mM solution. A 0.1 mM solution has λ_{max} 419, 540, 630 (sh). [d] Plus other equilibrium species, see text.

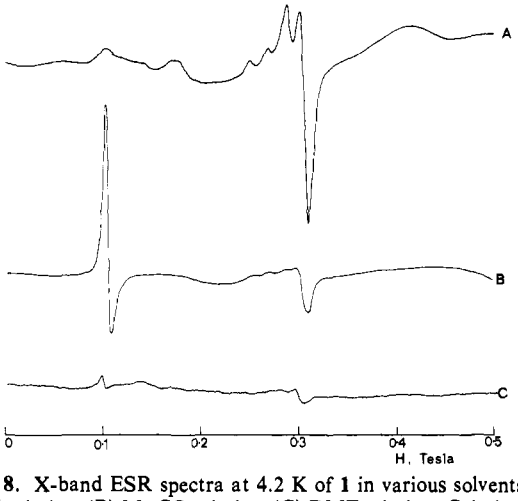

Figure 8. X-band ESR spectra at 4.2 K of **1** in various solvents: (A) MeCN solution, (B) Me_2SO solution, (C) DMF solution. Solutions were approximately 5 mM. Relative signal amplitudes A:B:C were 1:0.5:6.

This behavior is seen in other $[Fe(P)XCu(N_4)]^{2+}$ systems,[15] and we have shown that the excess base sequesters the Cu^{2+} from the (P)–(N_4) ligand system.

In acetonitrile solution, although the room-temperature visible spectrum and magnetic moment remain similar to the aforementioned solvent systems, the ESR spectrum at 4.2 K is quite different (Figure 8A) and can be interpreted in terms of a low-spin Fe(III) spectrum (g_z = 3.55, g_y = 2.14, g_x = 1.38) superimposed on a tetragonal Cu(II) spectrum ($g_{\parallel}$ = 2.25, $g_{\perp}$ = 2.05). These signals are of lower intensity (~20%) when compared to isolated low-spin iron(III) porphyrin or copper(II) signals and are unobservable above ~40 K. We attribute this to dipolar relaxation between the two metal centers, showing little or no magnetic superexchange interactions as observed for the high-spin Fe(III) case $[Fe(P)ClCu(N_4)]^{2+}$ studied previously.[8a,15] These observations are consistent with the structure indicated in Table V where the cyanide is no longer in a bridging position but is located outside the "pocket", and a nonbridging solvent molecule occupies the position between the two metal ions. A similar ESR spectrum is seen in solutions of the chloroiron(III) complex $[Fe(P)ClCu(N_4)](ClO_4)_2$ in this solvent, although the g values of the Fe(III) signals are slightly different, (g 3.58, 2, 1.36), which is to be expected on replacing a CN^- ligand with Cl^- (or CH_3CN).

In Me_2SO solution a similar rationale can explain the appearance of typical high-spin Fe(III) and Cu(II) signals at 4.2 K (Figure 8B). Again the intensity of these signals is low, and the appearance of a broad resonance around g 1.1 suggests an equilibrium situation, perhaps involving such species as $NC\overline{FeMe_2SO}\ CuMe_2SO$, $Me_2SO\overline{FeMe_2SO}\ CuMe_2SO$ (or CN^-), and a ferromagnetically coupled $Me_2SO\overline{FeCNCu}Me_2SO$.[38]

In DMF solution, on the other hand, the ESR spectrum is essentially featureless down to 4.2 K (Figure 8C). (A small signal at g ~6 integrating for <0.5% of a high-spin Fe(III) is attributed to an impurity.) Given that the visible spectrum and the 300 K moment are unchanged from the previous solvents and the rigidity of the (P)–(N_4) ligand, which effectively maintains a metal–metal distance of ca. 5.0 Å, an ESR silent species can arise in two ways: (a) through antiferromagnetic coupling between the low-spin Fe(III) and Cu(II), leaving the $S' = 0$ state lowest in energy and the $S' = 1$ state completely depopulated at 4.2 K or (b) through ferromagnetic coupling with a doublet ground state and an excited singlet state at an energy significantly higher than the microwave quantum.

We consider case a first. A 300 K magnetic moment of 3.5 μ_B restricts any coupling $-J$ to quite small values. A small value of $-J$ is not excluded, since a Boltzmann population of the $S' = 1$ state at temperatures much higher than ~30 K would not result in an observable ESR signal because of spin–spin relaxation broadening, as has been observed above and in other Fe/Cu complexes of this[8a] and related[8b] ligand systems. Since this coupling requires a bridging CN^- ligand, the question that now remains is how to account for a change from ferromagnetic to antiferromagnetic coupling within apparently similar structures (See Table V).

Ginsberg,[23] Martin,[39] Kahn,[40] and Hendrickson[41] have shown that the exchange coupling in bridged systems is made up of antiferromagnetic and ferromagnetic contributions, with the resultant sign of J dependent on the relative contributions of the overlap pathways involving atomic or molecular orbitals on the bridging group with d orbitals on the metal ("kinetic" and "potential" exchange[23]). In Figure 1, if the Cu—N(pyridine) directions are defined as x,y and the Cu—N≡C direction as z, then the Cu($d_{x^2-y^2}$) magnetic orbital will not overlap the σ orbital on the CN^- and only weakly overlap with the π^* orbital. At the Fe end of the bridge, the d_{xz} (or d_{yz}) magnetic orbital (from Mössbauer and ESR evidence, vide infra) will likewise only interact with the π^* orbitals on the CN^- and only weakly with the σ orbital. Although the exchange pathways are not strong and well-defined, the predominant interaction between the two metals

(38) Also noteworthy is the fact that the MCD spectrum of **1** at 295 K in Me_2SO shows only typical low-spin Fe(III) bands (Thomson, A. J., personal communication). The appearance of high-spin ESR signals at 4.2 K again points to a temperature dependent equilibrium. Other $(Me_2SO)_2Fe^{III}$ porphyrins have been shown to be high spin; see, for example: Mashiko, T.; Kastner, M. E.; Spartalian, K.; Scheidt, W. R.; Reed, C. A. *J. Am. Chem. Soc.* **1978**, *100*, 6354.

(39) Martin, R. L. In "New Pathways in Inorganic Chemistry"; Ebsworth, E. A. V., Maddock, A. G., Sharpe, A. G., Eds.; Cambridge University Press: Cambridge, England, 1968; Chapter 9, p 175.

(40) Kahn, O. *Inorg. Chim. Acta* **1982**, *62*, 3.

(41) Duggan, D. M.; Hendrickson, D. N. *Inorg. Chem.* **1973**, *12*, 2422. Duggan, D. M.; Barefield, E. K.; Hendrickson, D. N. *Ibid.*, **1973**, *12*, 985.

Table VI. Comparison of Electronic Features of **1**, Bovine Cyano-oxidase, and Bacterial Cyano-oxidase (a_3 Sites in Oxidized Form)

	bovine cyano-oxidase[6,44]	bacterial cyano-oxidase[1]	**1**
Fe(III) spin state	$S_{Fe} = {}^1/_2$	$S_{Fe} = {}^1/_2$	$S_{Fe} = {}^1/_2$
exchange coupling	ferromagnetic	ferromagnetic	weakly ferromagnetic
ESR (oxidized form) at 4.2 K	silent	silent	active, triplet spectrum
ESR (partially reduced, heme *a* site)	g_{Fe} 3.58, 1.56, 1.0		g_{Fe} 3.6, 2.06, 1.19 ($[Fe(P)CN(N_4)]^{2+}$)
Mössbauer (4.2 K), zero field	*a*	δ 0.28 mm s^{-1}, ΔE = 1.25 mm s^{-1}	δ 0.24 mm s^{-1}, ΔE = 1.87 mm s^{-1}
Mössbauer (4.2 K), applied field	*a*	broadening	broadening
ground state	$S' = 1$, $M_s = \pm 1$, zfs ca. 10 cm^{-1}	$S' = 1$, $M_s = \pm 1$,, zfs ca. 10 cm^{-1} small splitting of $M_s = \pm 1$ levels in zero field	$S' = 1$, $M_s = \pm 1$ ($S' = 0$ close by), zfs ca. 0.32 cm^{-1} small splitting of $M_s = \pm 1$ levels in zero field
exchange contributions	isotropic + axial splitting of $S' = 1$ state (J, D, and small E terms)	isotropic + anisotropic + asymmetric (J, D, E terms)	isotropic + anisotropic + dipole–dipole (J, J^{zz}, r terms)

[a] Similar to bacterial oxidase; see references to unpublished work in footnote 7 of ref 7.

is via orthogonal bridge orbitals, leading to net weak ferromagnetic coupling and an $S' = 1$ ground state. Changes in solvation of the Cu and Fe centers in DMF might affect the nature of the ground-state orbitals on the metal ions, which would influence the superexchange pathways in what is already a delicately balanced situation. This, together with the dominant effects of dipolar coupling described earlier, could well lead to a change in the resultant exchange interaction.

Case b is similar to that proposed for the CN^--oxidized form of cytochrome oxidase, based on MCD[6] and Mössbauer[7] measurements and discussed further below (Conclusion). The observance of an ESR signal in an $S' = 1$ system depends, inter alia, on the magnitude of the zero-field splitting D. In the oxidase, it is proposed that a predominantly axial distortion leaves the doublet $M_s = \pm 1$ as the ground state and the $M_s = 0$ component as the excited state, at least 10 cm^{-1} higher in energy. In the absence of any rhombic field and given the microwave quantum at X-band frequency, ESR signals are very weak or nonobservable because the transitions are spin forbidden. A sizeable rhombic splitting would make their observation even less likely. This may be compared with the solid state or $CHCl_3$–MeOH solutions of the present complex. In these cases, with H_2O, MeOH, or 1-MeIm as axial ligands, a small value of J and of the zero-field splitting of the triplet state allows an observable ESR spectrum. It is possible that alteration of the ligand field symmetries in DMF may lead to an axial distortion sufficiently large to wipe out the ESR signals. In the absence of more data, such as low-temperature solution susceptibilities or MCD measurements, we are unable to decide between cases a and b at this stage.

Conclusion

Since one of the initial aims of preparing and studying binuclear iron–copper porphyrins was to try to mimic the electronic features of the heme a_3–Cu_{a3} site in cytochrome oxidase, we look now at how the properties of the present cyanide-bridged complex compare with the cyanide-inhibited enzyme. There is apparently conflicting evidence based on the one hand on susceptibility measurements[3,4] and on the other on MCD[6] and more recent Mössbauer results,[7] as to the nature of the magnetic coupling between Fe(III) and Cu(II) in the a_3 site of the oxidase. However, Palmer and co-workers,[3,4] who initially concluded from susceptibility measurements the existence of weak antiferromagnetic coupling, have recently deferred their interpretation[42] in favor of the strongly ferromagnetic coupled model used by Thomson and Greenwood[6] to explain their low-temperature MCD and magnetization measurements on the mammalian enzyme. Since the completion of the present work, a Mössbauer and ESR study of a bacterial oxidase from *Thermus thermophilus* by Münck, Fee, et al.[7] has appeared. Using ^{57}Fe-enriched enzyme, this group has been able to obtain well-resolved spectra compared to the early work on the mammalian form[43] and have demonstrated a close similarity between the enzymes from the two sources. Their work confirms that the cyanide forms of both the oxidized bacterial and bovine enzymes appear to exist in single well-defined electronic states, compared to the heterogeneous forms now recognized in the a_3 site of the resting oxidized enzyme.[2d] Further, and of particular relevance to the present model study, they agree with the conclusions of Thomson and Greenwood[6] that there is strong ferromagnetic coupling between $S = {}^1/_2$ Fe and $S = {}^1/_2$ Cu producing an $S' = 1$ ground state. The pertinent features of the oxidized cyanide form of the bacterial and bovine enzymes and the present model complex are summarized in Table VI.

In general terms, it can be seen that the properties of $[Fe(P)CNCu(N_4)](ClO_4)_2$ correlate reasonably well with those of the a_3 enzyme site, demonstrating the effectiveness of the porphyrin complex as a working model. Since the sign of the exchange coupling, i.e., positive J, is intimately related to the superexchange pathways provided by a bridging CN^- ligand, we would postulate that an Fe^{III}–CN–Cu^{II} bridge exists in the a_3 site of the enzyme.

There are of course differences in detail, not the least of which is the lack of an ESR signal from the a_3 site of the enzyme even at temperatures as low as 4.2 K. There are a number of possible explanations for ESR silence in the enzyme compared to the triplet spectrum displayed by the present model. One possibility is that low- and high-field lines are in fact present but too weak to be recognized due to dilution effects and the superposition of heme *a*, Cu_a (and heme c_1) lines; this seems unlikely in view of the spectral resolution obtained in partially reduced cyano and other forms of the enzyme.[7,44] Extreme line broadening and lack of signals as a result of unsuitable relaxation times would be unlikely, at least in the bacterial enzyme, in view of the hyperfine structure observed in the Mössbauer spectrum in a small applied magnetic field.[7] Thomson et al.[6] explained the ESR silence in terms of a large zero-field splitting between the $M_s = \pm 1$ doublet and $M_s = 0$ level of ca. 10 cm^{-1}, leading only to forbidden $\Delta M_s = 2$ transitions from the $M_s = \pm 1$ components. This large zero-field splitting contrasts with the small splitting of ca. 0.32 cm^{-1} shown in Figure 7, which we have shown can give rise to ESR lines of the type exhibited by our weakly coupled model. Münck, Fee, et al.[7] have refined this picture somewhat in the case of the bacterial cyanide-treated oxidase by noting that rhombic symmetry can lead to a splitting of the $M_s = \pm 1$ levels in zero field perhaps by as much as 0.3 cm^{-1}, which, in combination with a large axial

(42) Wilson, L. J., personal communication (March, 1983).

(43) Lang, G.; Lippard, S. J.; Rosen, S. *Biochim. Biophys. Acta* **1974**, *336*, 6.

(44) Johnson, M. K.; Eglinton, D. G.; Gooding, P. E.; Greenwood, C.; Thomson, A. J. *Biochem. J.* **1981**, *193*, 699.

splitting, could well lead to lack of any ESR transitions (at least at X-band frequency).

Assuming that the magnitude of zero-field splitting terms, which originate in the kinds of interactions shown in Table VI, determines the observance or nonobservance of lines, we are left with the intriguing question of what factors in the enzyme lead to ESR silence. One possibility is a difference in the Fe–Cu distances and/or bridging mode of the CN^- group. Another possibility is the differences in g-term anisotropies (and hence ligand-field symmetries) on the Cu and Fe centers in the cyano enzyme compared to our model system, influenced by structural or other features of the protein matrix. As noted earlier in the solution behavior section, it is possible to simulate such effects in a crude way in the ESR tube by using DMF as solvent for the $[Fe(P)CNCu(N_4)]^{2+}$ complex. On the other hand, solutions in $CHCl_3$–MeOH with or without added 1-methylimidazole exhibit ferromagnetic coupling and an ESR triplet spectrum, whereas MeCN or Me_2SO solutions show little or no coupling. Further elucidation of these subtle but important features may be solved by low-temperature solution magnetic susceptibility, MCD, magnetization, and Mössbauer measurements or ultimately by X-ray crystallographic studies.

Acknowledgment. We thank Paul E. Clark and Mark Irving for the Mössbauer spectra and John Pilbrow for discussions on ESR spectroscopy. Discussions with Andrew Thomson on some aspects of this work are also gratefully acknowledged. K.S.M. acknowledges support from the Australian Research Grants Scheme and the Monash University Special Research Fund.

Registry No. 1, 90148-73-5; $Fe(P)Cl(N_4)$, 90242-08-3; $Fe(P)\overline{CN(N_4)}$, 90148-74-6; $H_2O\overline{FeCNCu}(H_2O)$, 90148-76-8; $MeOH\overline{FeCNCu}(MeOH)$, 90148-78-0; $MeIM\overline{FeCNCu}(MeOH)$, 90148-80-4; $NC\overline{FeMeCN\ CuMeCN}$, 90148-82-6; $NC\overline{FeMe_2SO\ CuMe_2SO}$, 90148-84-8; $DMF\overline{FeCNCu}DMF$, 90148-86-0; $Fe(P)OH(N_4)$, 90242-09-4.

Supplementary Material Available: Table listing χ_M, μ_{eff} (μ_B), and temperature (K) data for compound **1** (1 page). Ordering information is given on any current masthead page.

Systematic Trends in Metalloporphyrin Optical Spectra

M.-Y. Rachel Wang[1] and Brian M. Hoffman*[2]

Contribution from the Department of Chemistry, Northwestern University, Evanston, Illinois 60201, and the Department of Chemistry, Whitworth College, Spokane, Washington 99251. *Received September 29, 1983*

Abstract: We report the effects of axial ligands (L) on the optical spectra of cobalt-substituted myoglobin, horseradish peroxidase, and cytochrome $P450_{cam}$. In addition, we present data for a series of octapyrrole-substituted zinc porphyrin complexes. The response of a metalloporphyrin to the change of ligand is more complicated than previously noted and is not the same for pyrrole-substituted porphyrins as it is for meso-tetraaryl-substituted compounds. Perturbations by the ligand not only shift the overall spectrum as previously observed but also systematically change the frequency difference between the Soret (B) and the α–β (Q) bands. The observed trends in band frequencies can nevertheless be readily understood within the four-orbital model of Gouterman. Interpretation of band intensities is less clear.

Metal-substituted hemoproteins provide an ideal system for studies of metalloporphyrin properties,[3] and in this paper we report the effects of axial ligands (L) on the optical spectra of cobalt-substituted myoglobin, horseradish peroxidase, and cytochrome $P450_{cam}$. In addition, we present optical data for a series of octasubstituted zinc porphyrins, namely, zinc meso-, octaethyl-, and protoporphyrin complexes; since zinc porphyrins bind only a single axial ligand, they also provide a convenient system for systematically studying the influences of axial ligation. Cobalt and zinc porphyrins each exhibit only a single spin state (Co ($S = {}^1/_2$); Zn ($S = 0$)),[4] so complications from spin changes are absent.

The general pattern of a normal metalloporphyrin spectra is well-known.[4] It typically exhibits two moderately intense bands, the so-called α–β bands ($\epsilon \cong 10^4\ M^{-1}\ cm^{-1}$), in the vicinity of ~550 nm and an extremely strong band, the Soret, in the vicinity of ~400 nm ($\epsilon \sim 10^5\ M^{-1}\ cm^{-1}$) see Figure 1). In first approximation, these bands can be considered as π–π^* excitations localized on the porphinato macrocycle, and the overall nature of the spectra can be explained by reference to Gouterman's "four-orbital" mode[5,6,7] shown in Figure 2. This model focuses on transitions from the two highest occupied porphyrin π-molecular orbitals (a_{2u} and a_{1u} in D_{4h} symmetry) into the lowest pair of unoccupied MO's (e.g., in D_{4h} symmetry). The $a_1 \rightarrow e$ and $a_2 \rightarrow e$ excitations give rise to four excited configurations which are equivalent in pairs. They undergo pairwise configuration interaction to give the excited state that correspond to the Soret, or B, band, and the α–β, or Q, excitations. These excited configurations and resulting configuration mixed states are shown in Figure 2B.

The need for a detailed understanding of porphyrin spectra has led to the systematic correlation of spectra from complexes with different metals, peripheral substituents, and axial ligands.[4,8–12] These studies have shown that the α–β and Soret bands undergo frequency shifts in response to variations in metal and/or axial base and that the shifts correlate with variations in extinction

(1) Department of Chemistry, Whitworth College, Spokane, WA 99251.
(2) Northwestern University.
(3) Hoffman, B. M. In "The Porphyrins"; Dolphin, D., Ed., Academic Press: New York, 1978; Vol. III.
(4) Gouterman, M. In "The Porphyrins"; Dolphin, D., Ed.; Academic Press: New York, 1978; Vol. III.
(5) Gouterman, M. *J. Mol. Spectrosc.* **1961**, *6*, 138–163.
(6) Gouterman, M.; Wagniere, G. H.; Snyder, L. C. *J. Mol. Spectrosc.* **1963**, *11*, 108–127.
(7) Spellane, P. J.; Gouterman, M.; Antipas, A.; Kim, S.; Liu, Y. C. *Inorg. Chem.* **1980**, *19*, 386.
(8) Gouterman, M. *J. Chem. Phys.* **1959**, *30*, 1139–1161.
(9) Zerner, M.; Gouterman, M. *Theor. Chim. Acta* **1960**, *4*, 44–63.
(10) Antipas, Y. A. Ph.D. Thesis, University of Washington, Seattle, WA, 1979.
(11) Nappa, M.; Valentine, J. S. *J. Am. Chem. Soc.* **1978**, *100*, 5075–5080.
(12) Gouterman, M.; Schwartz, F.; Smith, P. D.; Dolphin, D. *J. Chem. Phys.* **1973**, *59*, 676.

0002-7863/84/1506-4235$01.50/0